



DOI: 10.34910/MCE.101.12

Silica concrete compressive behavior under alternating magnetic field

A. Safari Tarbozagh, O. Rezaifar*, M. Gholhaki

Department of Civil Engineering, Semnan University, Semnan, Iran

* E-mail: orezayfar@semnan.ac.ir

Keywords: Alternating Magnetic Field (AMF), concrete, silica sand, compressive strength, magnetic circuit

Abstract. Due to the importance of inventing new techniques capable of enhancing concrete structural properties while reducing environmental issues associated with CO₂ emissions in concrete industry, which preoccupies environmental scientists, a novel investigation was performed on feasibility of benefitting from Alternating Magnetic Field (AMF) and silica particles to attain this goal. Hence, some experiments were conducted on cylindrical concrete specimens comprising different silica sand contents of up to 10 %, wherein the influence of exposing fresh and hardened concrete to AMF of frequency 50 Hz and density 0.5 Tesla (T) on compressive strength of 7 and 28-day specimens was evaluated. For this, a specialized test setup was assembled such that the specimen could be subjected to compressive force and AMF, simultaneously. It was found that AMF can improve concrete compressive strength, where this technique is more efficient as to exposing hardened concrete. What was significant about the results was the fact that adding silica sand not only improved concrete mechanical strength but also considerably enhanced the effectiveness of AMF in increasing concrete compressive strength, when applied to hardened concrete. For instance, replacing 10 % of cement content with silica sand increased compressive strength of 28-day specimens by 8.4, but adding 10 % silica sand along with exposing specimens to AMF yielded an increase of nearly 21 % in real-time. Thus, developing this method can result in a new generation of smart constructions. Moreover, by adding 10 % silica sand, the emission of carbon dioxide, a greenhouse gas, reduces by 10 percent while significantly enhancing compressive strength.

1. Introduction

Nowadays, the need for improving concrete properties, such as workability and compressive, tensile and flexural strength has resulted in the invention of numerous ways, which are generally divided into two categories; the first is associated with using additives, such as nano- or micro-particles in concrete. The second is equipping concrete by non-cementitious phenomena, saying magnetic fields and electricity.

As to methods that use additives in concrete, the primary aim is to enhance concrete strength by replacing a proportion of cement constituent with other particles. This not only improves concrete structural properties but also reduces adverse environmental effects of using high cement content in concrete, which preoccupies environmental engineers. One of such cementitious admixtures, which has widely been studied according to technical literature, are silica particles. Recently, the use of nano- and/or micro-silica has been widely expanded because of their capability in enhancing mechanical properties and microstructure of concrete due to pozzolanic reaction between micro-silica and Ca(OH)₂ [1, 2]. Some of these improvements are increase in compressive, tensile and flexural strength, reduction of concrete setting time and permeability, immunity against chemical and corrosive reactions [3–6].

Wang et al. investigated the effect of nano-silica on hydration and microstructure of alkali-activated slag. They concluded that adding nano-silica improves concrete compressive strength, microscopic morphology and hydration [7]. Assaedi et al. studied the influence of methods for mixing nano-silica on microstructural evolution and performance of Geopolymer paste prepared with fly ash. They found that concrete strength improvement and optimization in microstructure depends on hydrated calcium silicate and hydrated calcium alumino-silicate gel [8]. Regarding silica sand, Mithaq investigated compressive strength improvement using

Safari Tarbozagh, A., Rezaifar, O, Gholhaki, M. Silica concrete compressive behavior under alternating magnetic field. Magazine of Civil Engineering. 2021. 101(1). Article No. 10112. DOI: 10.18720/MCE.101.12



This work is licensed under a CC BY-NC 4.0

silica sand [9]. Sayed et al. found that substituting silica sand for a proportion of cement enhances compressive and flexural strength by 55.7 % and 46.9 %, respectively, while reducing workability [10].

With regard to using phenomena other than additives in concrete, one of the well-known methods is enhancing concrete elements performance through magnetic fields and/or electricity, where studies in this field are divided into two major categories; a) enhancing concrete mechanical properties through applying magnetic field to concrete constituents in fresh state and b) benefiting from magnetism and electricity in real time controlling of smart structures behavior.

Recently, improving concrete properties through magnetizing its constituents has drawn the attention of many structural engineers. One method is preparing magnetic concrete via magnetic treatment of water, where water is exposed to a high power magnetic field. This method was first suggested by Lorenz in 1902 for the first time. When water is exposed to magnetic field, the size of its molecules increases [11]. Hence, its properties, such as surface tension, temperature, PH, permeability, solubility and specific weight are influenced [12, 13].

Most research studies on concrete reported that using magnetic water increases workability and compressive strength by 10 to 25 % [14–18]. Bharath et al. [19] concluded that mixing concrete with magnetized water improves workability of concrete comprising copper slag by 5 %. According to a work done by Gholhaki et al. [20], magnetic treatment of water improves flowability and viscosity of self-compacting concrete. According to the work of Ghorbani et al. [21] magnetic water considerably improves concrete microstructure and makes concrete more consistent compared with ordinary concrete. Another study done by Su et al. [16] revealed that magnetized water increases compressive strength of mortar comprising blast-furnace slag. But, the extent of such effect depends on magnetic field strength. This method was also found to have a positive influence on concrete with Egyptian nano-alumina [14].

Not only magnetizing water but also exposing other concrete constituents has recently been investigated. Nair et al. exposed fresh concrete containing carbonyl iron powder to magnetic field. They said this technique affects concrete paste shear resistance but does not influence compressive strength [22]. In another study, different cement paste specimens of ages up to 7 days were subjected to static magnetic fields of up to 25.37 Gauss (1 Gauss= 10^{-4} T). It was concluded that magnetic field enhances Calcium Silicate Hydrate (CSH) gel constituent and improves its morphology [23].

Moreover, magnetic field and electricity have found their way into real time controlling of concrete elements behavior. In this regard, electromagnetism has been commonly used for performance monitoring in concrete elements [24], [25], where the apparatus mainly consists of sensors and actuators. Such systems are mainly based on smart materials, such as shape memory alloys [26–28], piezoelectric [29–31], fiber optics [32–35], and magneto-rheological materials[36]. Apart from applying electromagnetism in sensors and actuators systems, exposing concrete itself to magnetic field has recently been found to influence concrete performance in real time, which can be considered as a base for a new smart construction system [37–41]. Abavisani et al. [37] studied the influence of exposing fresh and hardened concrete to Alternating Magnetic Field (AMF) on its properties. They observed that AMF has a positive effect on concrete compressive strength as long as AMF is applied to hardened concrete. They also subjected some small-scale RC beams to AMF and/or alternating current (AC) electricity[38]. They found that this technique affects flexural properties of the beams, such as load-bearing capacity, flexural stiffness, ductility and deflection. For instance, exposing fresh concrete to AMF, when placing, enhanced ductility of RC beams by 15.4 % and subjecting hardened RC beams to AMF enhanced their ductility index by 135.8 %. In another study, Rezaifar et al. [39] Prepared some small-scale RC columns and subjected them to AMF and/or AC. It was found that load bearing capacity of the RC columns increased during AMF exposure but they became more brittle, on the other hand AC made them more ductile.

However, studies on the influence of AMF on concrete are still scarce and almost limited to plain concrete without admixtures. Hence, it is necessary to investigate further on this issue and evaluate the effect of AMF on other concrete additives. This study aims to take this area further and evaluate the effectiveness of AMF in improving compressive strength of concrete containing other additives, which has not been studied before.

In this study, the influence of AMF on cylindrical concrete specimens containing silica sand as admixture in the ages of 7 and 28 days is evaluated. The study is divided into two; the effect of applying AMF to fresh concrete and the influence of exposing hardened concrete to AMF on compressive strength. Section 2 is devoted to explaining research method and practical issues about using AMF. Then in section 3, the experimental data will be presented and the effect of both silica and AMF on concrete compressive strength will be discussed. This is followed by discussing the advantages of this technique in terms of environmental benefits as well as designing issues. Since RC beams have an important role in structural ductility, which withstand transverse loading through interactions between compressive and tensile stresses in concrete and reinforcing bars, part of design advantages will be discussed as to RC beams. Finally, conclusions are presented in section 4.

2. Methods

2.1. Test program

In this investigation, the effect of AMF on compressive strength of concrete cylinders containing different proportions of silica sand was the target. Hence, 54 concrete samples, in total, were tested. The variables are as follows:

- The occasion when concrete is exposed to AMF. In this regard, specimens are categorized as:
 - Non-Magnetized (NM): where AMF is not applied to concrete
 - Pre-Magnetized (PrM): where AMF is applied to ready mixed concrete casted into mold
 - Post-Magnetized (PoM): where AMF is applied to hardened concrete as it is subjected to compressive force during the test.
- Silica sand content; the specimens are categorized into three groups containing silica sand contents of 0 %, 5 % and 10 % of the cement weight.
- Concrete age; concrete samples are divided into 7-day and 28-day specimens.

Specimens are labeled according to these variables. Each label is composed of three parts separated by full stops; the first one is related to variable I, which is NM, PrM or PoM. The second is a number connoting the percentage of silica concrete, which takes one of the amounts of 0,5,10. The last section identifies the age of concrete, which is either 7 or 28. All labels are presented in Table 1.

Table 1. Specimen labels.

AMF	Silica sand content (%)	Label	
		7-day specimen	28 days specimen
NM	0	NM.0.7	NM.0.28
	5	NM.5.7	NM.5.28
	10	NM.10.7	NM.10.28
PrM	0	PrM.0.7	PrM.0.28
	5	PrM.5.7	PrM.5.28
	10	PrM.10.7	PrM.10.28
PoM	0	PoM.0.7	PoM.0.28
	5	PoM.5.7	PoM.5.28
	10	PoM.10.7	PoM.10.28

2.2. Material Properties

In all specimens Portland cement type ii with a trade name of Shahroud Cement was used. The cement properties are listed in Tables 2 and 3. The water used was tap water. For aggregate with a diameter of less than 4.75 mm, sand was graded as per ASTM-C33 [42]. The grading diagram for sand constituent is shown in Fig. 1. Water absorption test was performed on sand and gravel and its results are listed in Table 4. In this study, silica sand of diameter less than 75 μm was utilized as a partial substituent for cement. The technical properties and proportions of the silica sand are presented in Table 5. To improve workability, a carboxylate superplasticizer under a trade name of PX-MIX was employed, where its properties are listed in Table 6.

For magnetization, an AMF equipment run by main electricity, generating a magnetic field of strength 0.5 Tesla (T) with a frequency of 50 Hz was employed. Due to the fact that steel molds have a high level of magnetic permeability, there would have been a huge magnetic leakage if fresh concrete had been magnetized in such molds. As a consequence, the amount of magnetic flux passing through ready mixed concrete would have been drastically reduced. Therefore plastic cylindrical molds of 20x10 cm with a thickness of 3 mm were used.

Table 2. Material Chemical proportions of the Cement (as a proportion of cement weight %).

SiO ₂	Al ₂ O ₃	Fe ₂ O ₃	CaO	MgO	SO ₃	Na ₂ O	K ₂ O	TiO ₂	P ₂ O ₅	Mn ₂ O ₃	Loss on ignition
21.11	4.42	3.96	63.36	1.51	2.61	0.38	0.51	0.28	0.19	0.07	1.6

Table 3. Mineral proportions of the Cement (as a proportion of cement weight %).

C ₃ S	C ₂ S	C ₃ A	C ₄ AF	Loss on ignition
54.7	19.3	5	12.5	8.5

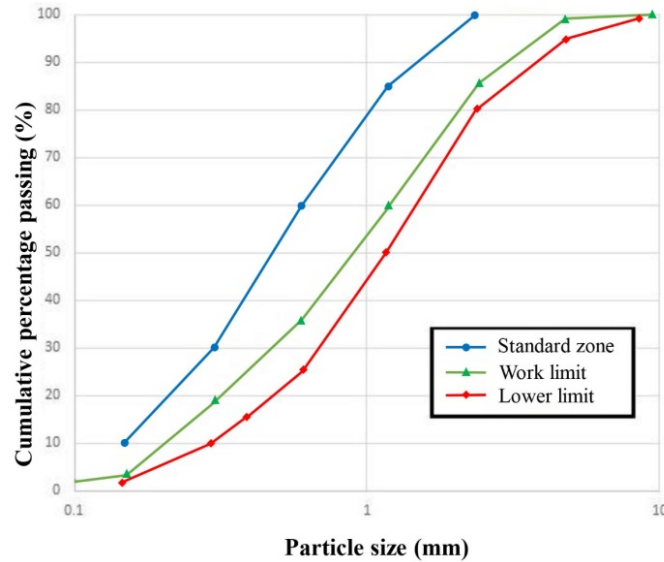


Figure 1. The aggregate grading diagram.

Table 4. The results of water absorption of aggregate.

	Weight of saturated aggregate with a dry surface (g)	Weight of aggregate after 24 h heated in oven (g)	Water absorption
gravel	504.1	498.5	1.1%
Sand	534.6	485.8	10%

Table 5. The silica sand properties.

Constituent	SiO ₂	Al ₂ O ₃	Fe ₂ O ₃	CaO	MgO	Na ₂ O	K ₂ O
Proportions (%)	98.27	0.48	0.12	0.18	0.08	0.63	0.24

Table 6. The superplasticizer properties.

Physical phase	Liquid
Color	Light yellow
Standard	ISIRI2930 & ASTM-C494
Specific weight	1.4 gr/cm ³

2.3. Magnetic circuit

For magnetizing concrete in this study a simple magnetic circuit was adopted, where the schematic formation of this circuit is illustrated in Fig. 2. This gapped circuit consists of a coil, a core of iron and an air gap where concrete specimens are placed and magnetized.

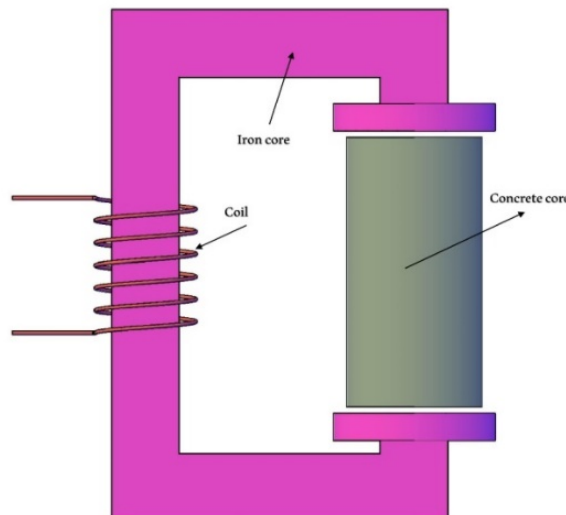


Figure 2. The gapped magnetic circuit designed for magnetizing the specimens.

When an element is subjected to a magnetic field, magnetic flux passes through it. The density of such flux is calculated as:

$$B = \frac{\phi}{A}, \quad (1)$$

where B is magnetic flux density measured (in T);

ϕ is magnetic flux measured in Weber (Wb);

A is cross-sectional area of the element (measured in m^2).

Magneto Motive Force (MMF) which represents the amount of magnetic forces along a circuit is follows:

$$F = NI, \quad (2)$$

where F , N , and I denote, MMF (measured in ampere-turn (At)), the number of the turns of the coil, and the current intensity running through the coil (in amperes (A)), respectively. Since in this study fixed amounts of I and N are adopted, MMF remains constant.

The reluctance of an element to allow magnetic flux through itself, which is called magnetic reluctance of the element, is calculated as:

$$R = \frac{l}{\mu A}, \quad (3)$$

where l represents the length of that element measured in (m);

A connotes the cross-sectional area of the element measured in (m^2);

μ is magnetic permeability of the material which the element is made of, measured in henries per meter ($H.m^{-1}$).

The magnetic flux running through the circuit (ϕ) is as:

$$\phi = \frac{F}{R_I + R_C}, \quad (4)$$

where R_I and R_C denote magnetic reluctances of iron and concrete elements, respectively.

Eqs. (3) and (4) are based on static magnetic field which is created by Direct Current (DC) electricity. As to AMF, these equations are modified as Eqs. (5) and (6).

$$Z_\mu = \frac{l}{\dot{\mu}S}, \quad (5)$$

$$\dot{\phi} = \frac{\dot{N}}{Z\mu_I + Z\mu_C}, \quad (6)$$

where Z_μ represents complex magnetic reluctance;

l denotes the length of the element measured in (m);

$\dot{\mu}$ is the complex magnetic permeability, which relates to the material quality;

S represents the cross-sectional area of the element;

$\dot{\phi}$ denotes the amplitude of magnetic flux;

\dot{N} is the amplitude of magneto motive force (MMF);

$Z\mu_I$ and $Z\mu_C$ stand for Z_μ of iron and concrete elements, respectively. The amounts of μ and $\dot{\mu}$ for iron are by far larger than those for concrete core. Therefore, R_C and $Z\mu_C$ are markedly larger than R_I and $Z\mu_I$, respectively. Considering Eqs. (4) and (6), since F and \dot{N} are fixed amounts, there is a sharp

decrease in magnetic flux only because of the concrete gap (R_C and/or $Z\mu_C$ are large numbers). Since the aim of the experiments in this study is to run as much magnetic flux across concrete specimens as possible, the smallest length for concrete cylinders (20 cm) was adopted as a way to keep magnetic reluctance of concrete as low as possible (according to Eqs. (3) and/or (5)). The simplified structure of the AMF generating equipment employed for magnetizing the specimens is shown in Fig. 3.

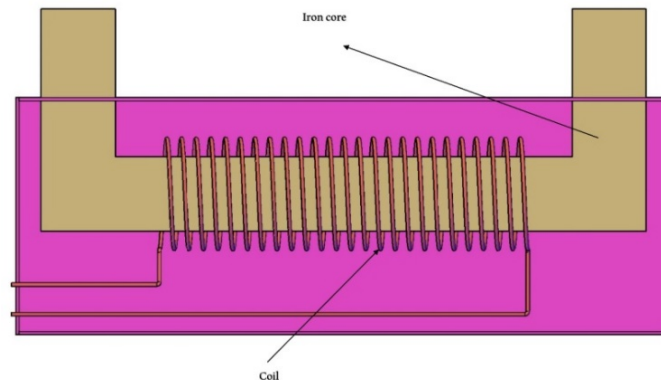


Figure 3. The AMF generator used for magnetization of the concrete samples.

2.4. Specimen preparation

After searching some articles working on silica concrete in literature and experimenting with different concrete proportions through trial and error, the best mix proportions as presented Table 7 were used. First, gravel and sand were combined with each other in a mixer. Then, a portion of the mix water, enough to render aggregates in a saturated-surface-dry (SSD) condition, was poured into the mixer and the mixture was stirred for about 1 min. Subsequently, cement (along with silica sand in case of 5 % and 10 % silica sand specimens) was added to the saturated aggregates. Meanwhile aggregates and cementitious constituents were mixed together, the rest of water content mixed with superplasticizer was poured, gradually, into the mixer. Totally, the mix procedure took around 3 to 4 min. Then, the concrete slump was performed on the freshly mixed concrete according to ASTM-C143 [43] to ensure a desirable slump (Fig. 4). Due to high specific surface area of silica, it has a water absorption capability, reducing slump of concrete. In this study, slump for all mix proportions was targeted to remain within the range of 5 to 10 cm.

After that, ready mixed concrete was placed into molds and compacted by a shaker table. For each type of specimens three samples were fabricated. Finally, PrM specimens were subjected to the AMF as shown in Fig. 5. As is seen in the figure, to ensure the coverage of magnetic flux across the entire of specimens, two rectangular prisms were put along two opposite sides of the mold. Fig. 6 shows the direction of AMF applied to the PrM specimens.

Concrete cylinders were demolded after 24 h. In order to prevent $\text{Ca}(\text{OH})_2$ from coming out of concrete the specimens were cured into saturated limewater until their compressive testing date.

Table 7. Mix proportions of specimens.

Specimen	Gravel (kg/m^3)	Sand (kg/m^3)	Cement (kg/m^3)	Silica sand (%)	Water (kg/m^3)	w/c	Superplasticizer (kg/m^3)	Slump (cm)
NM.0.7								
NM.0.28								
PrM.0.7	516	1204	400	0	180	0.45	0.8	9.4
PrM.0.28								
PoM.0.7								
PoM.0.28								
NM.5.7								
NM.5.28								
PrM.5.7	516	1204	380	5	180	0.45	0.87	8.6
PrM.5.28								
PoM.5.7								
PoM.5.28								
NM.10.7								
NM.10.28								
PrM.10.7	516	1204	360	10	180	0.45	0.98	5
PrM.10.28								
PoM.10.7								
PoM.10.28								

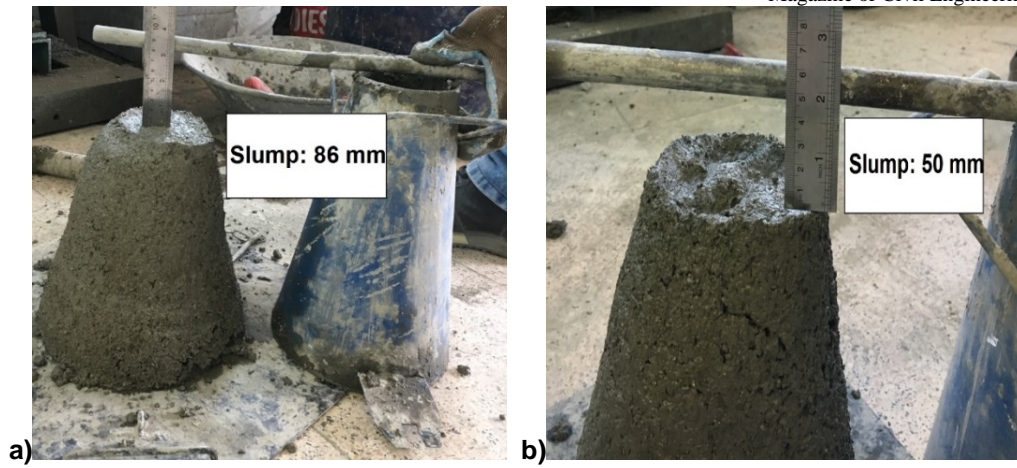


Figure 4. The slump test for: a) A specimen comprising 5 % silica sand
b) A specimen comprising 10 % silica sand.

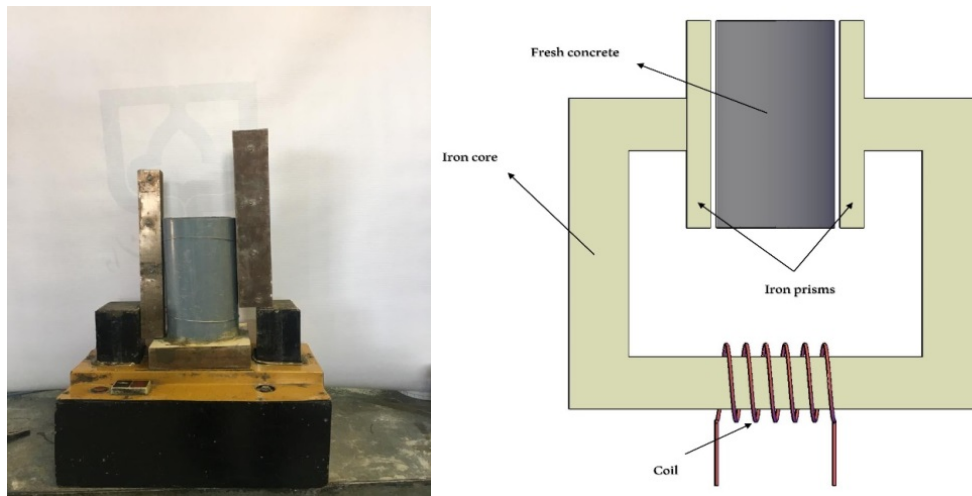


Figure 5. A PrM specimen subjected to AMF.



Figure 6. The direction of magnetization of PrM specimens.

2.5. Test procedure

The concrete cylinders were tested as per ASTM-C39 [44]. For testing the PoM specimens, a test setup was devised in a way that concrete could be subjected to both pressure and AMF, simultaneously, as shown in Fig. 7. As can be seen, the two terminals of the AMF generator were in touch with the upper and lower platens of the compression measuring apparatus. These specimens were exposed to AMF throughout the experiment. In fact this setup was used for testing all the three magnetic categories (NM, PrM, PoM) but only for PoM specimens was the AMF generator in work.

In order to make sure AMF did not affect digital sensors of measuring machine during testing of the PoM specimens, which renders test results unreliable, a non-digital compression equipment with the trade name Wykehaln Farrance was employed.

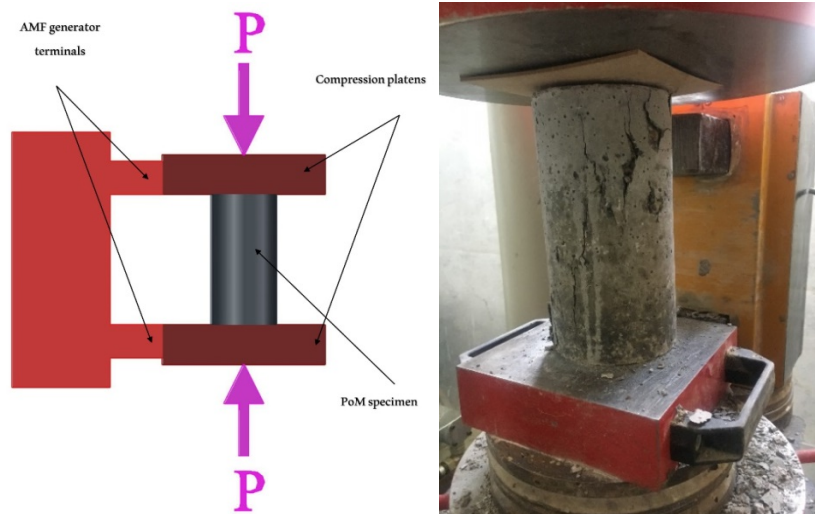


Figure 7. The test apparatus for specimens.

3. Results and Discussion

The compressive test results for 7-day and 28-day specimens are presented in Tables 8 and 9. In these tables compressive strength of NM.0.7 and NM.0.28 are regarded as a benchmark in order to better discuss the results.

Table 8. The compressive results of 7-day specimens.

AMF	Silica (%)	Specimen	Compressive strength			Enhancement relative to NM.0.7 (%)
			exact data	average	Standard deviation (σ)	
	0	NM.0.7	28.4,28.6,29.1	28.7	0.36	0
NM	5	NM.5.7	30.5,31,31.3	30.9	0.4	7.7
	10	NM.10.7	31.9,32.1,32.3	32.1	0.2	11.8
PrM	0	PrM.0.7	29.6,30,30.1	29.9	0.26	4.2
	5	PrM.5.7	31.9,32.4,32.6	32.3	0.36	12.5
	10	PrM.10.7	33.3,33.7,34.2	33.7	0.45	17.4
PoM	0	PoM.0.7	30,30.7,30.8	30.5	0.44	6.3
	5	PoM.5.7	33.3,33.8,34	33.7	0.36	17.4
	10	Pom.10.7	36,36.3,36.9	36.4	0.46	26.8

Table 9. The compressive results of 28-day specimens.

AMF	Silica (%)	Label	Compressive strength			Enhancement relative to NM.0.28 (%)
			exact data	average	Standard deviation (σ)	
	0	NM.0.28	38.7,39,39.6	39.1	0.46	0
NM	5	NM.5.28	39.7,39.9,40.4	40	0.36	2.3
	10	NM.10.28	41.9,42.6,42.7	42.4	0.44	8.4
PrM	0	PrM.0.28	40.2,40.4,40.9	40.5	0.36	3.6
	5	PrM.5.28	41,41.6,41.9	41.5	0.46	6.1
	10	PrM.10.28	43.7,44,44.6	44.1	0.46	12.8
PoM	0	PoM.0.28	41,41.1,41.8	41.3	0.44	5.6
	5	PoM.5.28	42.8,43,43.5	43.1	0.36	10.2
	10	PoM.10.28	47,47.1,47.5	47.2	0.26	20.7

2.6. The effect of adding silica sand

Since non-magnetized (NM) specimens were not exposed to AMF, these samples were adopted to discuss the influence of only silica sand content on compressive strength. The empirical data and approximate curves fitted to them for compressive strength enhancement of NM specimens comprising 0, 5 and 10 % silica sand, due to silica particles content, relative to the benchmark data are illustrated in Fig. 8. As is evident, with increase in silica sand constituent in concrete, the compressive strength of concrete increased, where maximum increases for 7-day and 28-day specimens were 11.8 % and 8.4 %, respectively, adding 10 % silica sand.

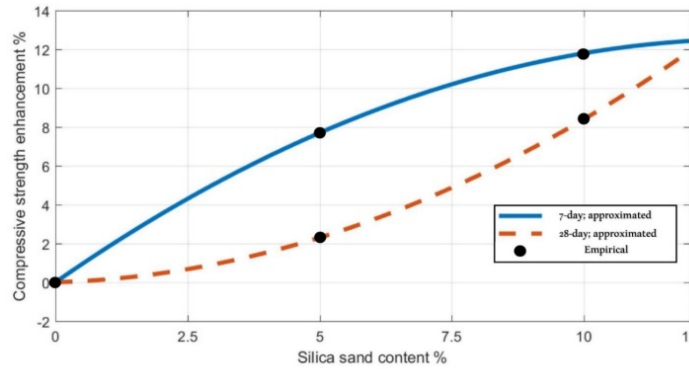


Figure 8. Compressive strength improvement for NM specimens due to adding silica sand: the experimental data and the cures fitted to them.

For better formulation of the effect of silica on compressive strength improvement, the enhanced extent of 7-day and 28-day NM specimens can be estimated through Eqs. (7) and (8), respectively, as a function of silica sand content. Note that R-square for both equations are 1.

$$E = -0.072S^2 + 1.9S + 1.83 \times 10^{-15} \quad \text{For the age of 7 days} \quad (7)$$

$$E = 0.076S^2 + 0.08S - 2.144 \times 10^{-15} \quad \text{For the age of 28 days} \quad (8)$$

Where E and S are compressive strength enhancement percentage and silica sand content (%), respectively.

As is seen, although the rate of compressive strength enhancement due to adding silica sand at percentages of this study is more significant as to 7-day concrete cylinders compared to the 28-day aged ones, which may be attributed to the fact that most of C_3SH in concrete is formed in the first days after concrete preparation [45], This rate for 7-day specimens is decreasing as silica sand content increases whereas the trend for 28-day concrete is reversed; at a silica content more that 10 % the enhancement of compressive strength in 28-day concrete would be more significant than 7-day one.

2.7. The effect of AMF

To discuss the effect of pre-magnetization and post magnetization on compressive strength, the enhancement data of NM specimens in Tables 8 and 9 are subtracted from the corresponding data of PrM and PoM specimens, respectively. The resultant data are visually presented in Fig. 9.

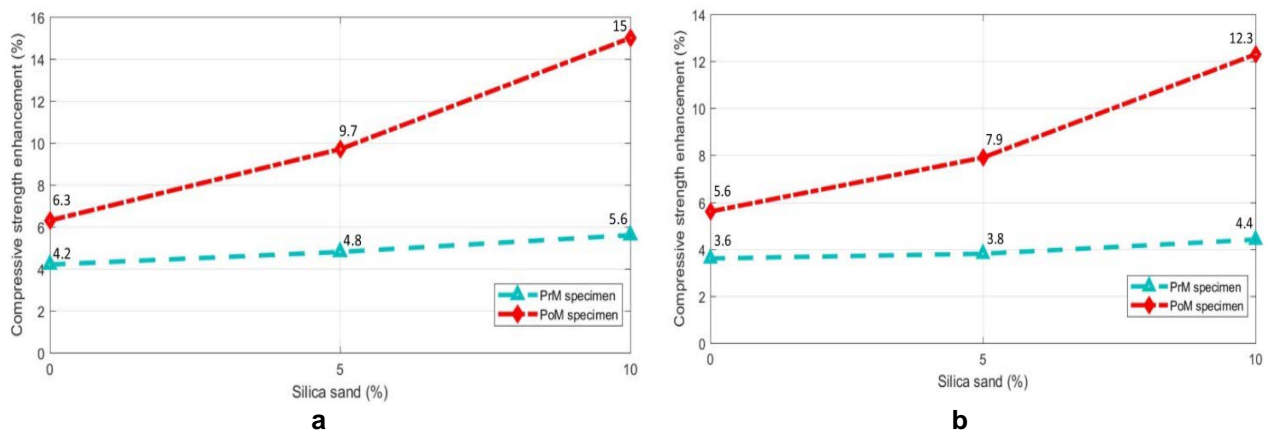


Figure 9. Enhancement of compressive strength for PrM and PoM specimens under the effect of only AMF: a) 7-day specimens, b) 28-day specimens.

In order for better realization of the issue, experimental data of compressive strength improvement along with the approximated curves fitted to them for PrM and PoM specimens of age 7 and 28 days are illustrated in Fig. 10.

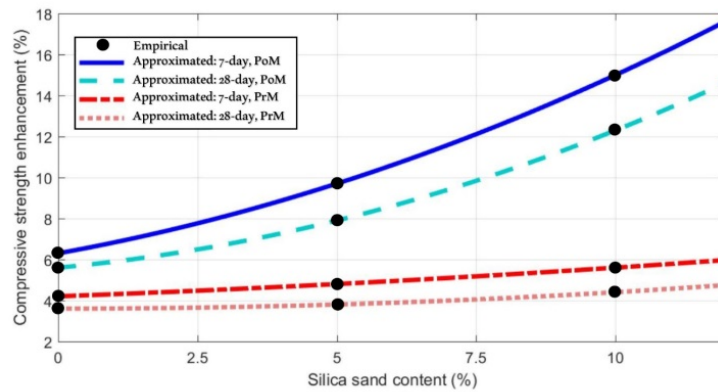


Figure 10. Compressive strength improvement for PoM and PrM specimens due to only AMF: the experimental data and the cures fitted to them.

All the approximated curves are cube functions as listed below, where the amount of R-square for all of them is 1.

$$E = 0.038S^2 + 0.49S + 6.3 \quad \text{7-day, PoM} \quad (9)$$

$$E = 0.042S^2 + 0.25S + 5.6 \quad \text{28-day, PoM} \quad (10)$$

$$E = 0.004S^2 + 0.1S + 4.2 \quad \text{7-day, PrM} \quad (11)$$

$$E = 0.008S^2 - 3.979 \times 10^{-16} S + 3.6 \quad \text{28-day, PrM} \quad (12)$$

A comparison of the approximate curves reveals that the effectiveness of AMF for 7-day specimens is more significant than 28-day ones. Moreover, with increase in silica sand proportions, AMF is more effective in enhancing concrete compressive strength, where the greatest increase for 7-day and 28-day samples (15 and 12.3 %, respectively, according to Fig. 9). Resulted from adding 10 % silica sand.

The most obvious fact is that post-magnetization has been by far more effective in improving concrete compressive strength compared with pre-magnetization. This may be rooted in the fact that silica is a diamagnetic substance. Such materials contain charged microparticles that can be influenced by an external magnetic field but as soon as it disappears the material reverts to its regular condition. When diamagnetic particles are subjected to a magnetic field they are repelled back because a magnetic field is induced in them in the opposite direction (Fig. 11) [46]. Compressive testing of PrM samples was carried out in a situation that AMF was not present and most of charged particles had reverted to their original position but testing of PoM specimens were conducted in the presence of AMF. That is, most of charged particles were influenced by magnetic field and this may be reason why PoM specimens showed a greater improvement compared to PrM ones.

According to Fig. 9, post magnetization enhanced compressive strength of 7-day concrete with 10 % silica sand by 15 % while pre-magnetization increased its strength up to only 5.6 %. Likewise, the figures for 28-day samples are 12.3 and 4.4, respectively.

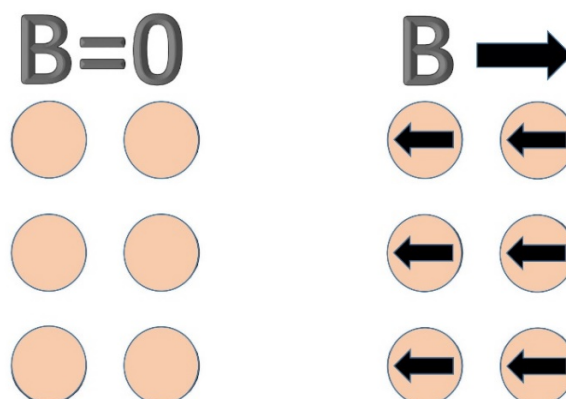


Figure 11. The orientation of diamagnetic particles in the presence and absence of magnetic field.

2.8. Advantages of this techniques

2.1.1. Environmental advantages

The advantages of adding silica sand as a partial replacement for cement in this study can be discussed environmentally. To explain, the cement industry, is one of the two major CO₂ producers, accounting for up to 8 % of man-made emissions of this gas throughout the world. The amount of CO₂ emitted due to concrete fabrication depends, directly, on cement content in concrete mixture. For preparation of one ton of cement, 900 kg of CO₂ are released, which amounts to 88 % of the emissions for the average concrete mix [47, 48]. Therefore, replacing a portion of cement with other additives is justifiable and a wide variety of such admixtures as silica particles has been established in concrete industry. According to Table 9, replacing 10 % percent of cement content with silica sand and then post-magnetizing it not only enhanced compressive strength of concrete by more than 20 %, but also resulted in a reduction of 10 % in CO₂ emissions.

2.1.2. Advantages of post-magnetization: theoretical discussion

As stated earlier exposing hardened concrete can improve concrete compressive strength as long as magnetic field is present. This implies that this technique could be a base for developing a new model for smart concrete structures where their behavior in the presence of powerful dynamic forces, saying earthquake, can be controlled by AMF. Therefore, in this section some advantages of this technique are theoretically discussed according to ACI [49].

- *Controlling structural behavior of concrete element*

A wide variety of patterns for relationship between stress and strain of concrete have been proposed. One of the most well-known models is the one suggested by Hognestad [50] in which at any stage of loading before reaching maximum load bearing capacity of concrete, f'_c , stress in concrete is calculated as a function of strain as follows:

$$f_c = f'_c \left[2 \frac{\varepsilon_c}{\varepsilon'_c} - \left(\frac{\varepsilon_c}{\varepsilon'_c} \right)^2 \right] \quad (13)$$

where f_c is stress in concrete.

ε_c is strain in concrete.

ε'_c is the strain corresponding to f'_c .

After hitting the peak point (f'_c) stress is calculated by a linear function as:

$$f_c = f'_c \left[1 - 0.15 \left(\frac{\varepsilon_c - \varepsilon'_c}{\varepsilon_{cu} - \varepsilon'_c} \right) \right] \quad (14)$$

where ε_{cu} represents the ultimate strain in concrete.

According to the test results, magnetizing hardened 28-day 10 % silica sand concrete (PoM.10.28) enhanced its compressive strength by 12.3 % ($f'_c \Rightarrow 1.123f'_c$). According to ACI [49] formulas ε'_c is proportional to $\sqrt{f'_c}$. As a result, ε'_c turns into $\sqrt{1.123}\varepsilon'_c$. Modifying Eq. (13), the stress-strength relation for a PoM.10.28 specimen is as:

$$f_c = 1.06f'_c \left[2 \frac{\varepsilon_c}{\varepsilon'_c} - \frac{1}{1.06} \left(\frac{\varepsilon_c}{\varepsilon'_c} \right)^2 \right] \quad (15)$$

Hognestad diagrams for PoM.10.28 and NM.10.28, where AMF is 0.5T and 0T, respectively, are illustrated in Fig. 12(a) (Note that since NM.10.28 specimens were not exposed to AMF, the enhancement of compressive strength due to AMF for them is 0. Therefore the diagram associated with AMF= 0T is drawn according to Eq. (13), where ε'_c is assumed to be 0.002).

If a concrete element in a smart structure is designed in a way that when strain (ε_c) reaches a point close to ε'_c (P_1 in Fig. 12(b)), an AMF generating actuator turns on. In this case, a transition from P_1 to P_2 is

expected, theoretically. But due to appearance of micro-cracks, it is likely to see a transition from P_1 to a point, saying P_3 , where the element can withstand a stress equal to or even more than f'_c of the diagram for AMF=0T, without reaching ε'_c . This means that there is an increase in modulus of elasticity and stiffness by moving from P_1 to P_3 . After that, the diagram continues towards P_4 and then collapses at P_5 .

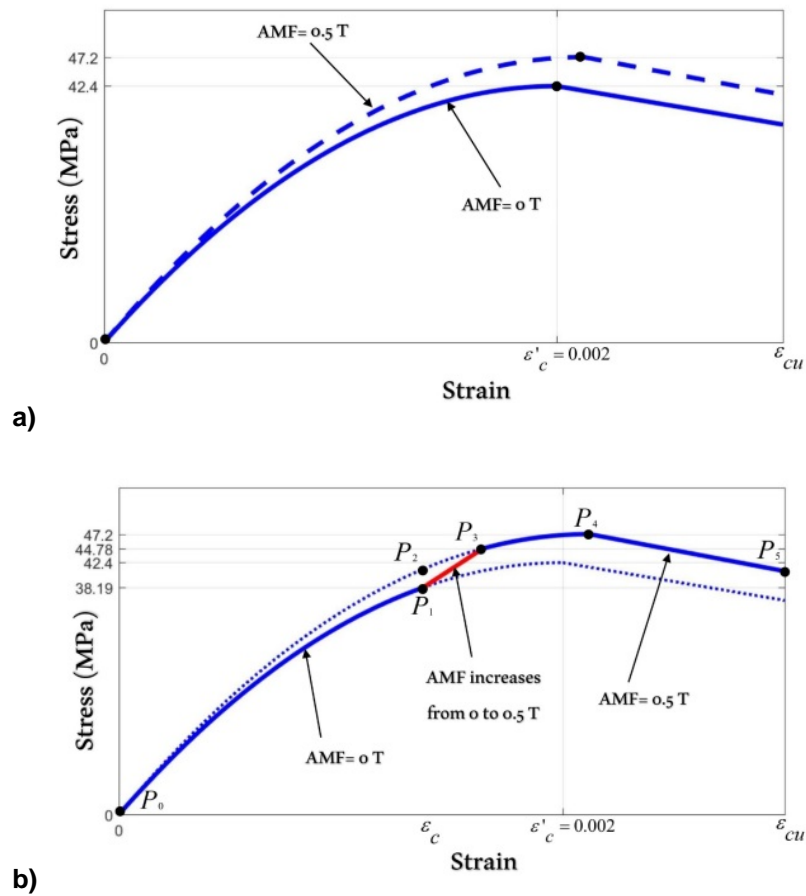


Figure 12. a) Hognestad curves for a smart concrete in the presence and absence of AMF, b) The change in structural behavior of this element due to applying AMF.

- *Moment strength of reinforced concrete beams*

For RC beams the nominal moment strength (M_n) is obtained as:

$$M_n = \rho f_y b d^2 \left(1 - 0.59 \rho \frac{f_y}{f_c} \right), \quad (16)$$

where ρ , b and d stand for, respectively, tension bar ratio, the width of the beam and the effective depth of it. Regarding the increase in compressive strength of 15 and 12.3 % for 7-day and 28-day aged concrete, respectively, containing 10 % silica sand, due to AMF exposure, the nominal moment strength for them is increased and calculated as:

$$M_n = \rho f_y b d^2 \left(1 - 0.51 \rho \frac{f_y}{f_c} \right) : \quad \text{For the age of 7 days} \quad (17)$$

$$M_n = \rho f_y b d^2 \left(1 - 0.52 \rho \frac{f_y}{f_c} \right) : \quad \text{For the age of 28 days} \quad (18)$$

- *Minimum reinforcement ratio*

The minimum reinforcement ratio for RC beams is obtained as:

$$\rho_{\min} = \frac{\sqrt{f_c}}{4 f_y} \geq \frac{1.4}{f_y} \quad (19)$$

where f'_c and f_y represent concrete compressive strength and reinforcing bars' yield strength, respectively, in MPa. In case f'_c exceeds 31 Mpa, ρ_{\min} is obtained as $\frac{\sqrt{f'_c}}{4f_y}$ where minimum reinforcement is proportional to $\sqrt{f'_c}$. According to Fig. 9(b), post-magnetizing enhanced compressive strength of 28-day specimens containing 10 % silica sand by 12.3 %. As a result ρ_{\min} can be reduced by 6 % if the concrete beam is subjected to AMF in the presence of strong dynamic forces.

- *Ductility of concrete beams*

It is well known that the higher the compressive strength, the more ductile RC beams are [51, 52]. As a result, exposing reinforced concrete elements in some critical areas of smart constructions to AMF, when strong cyclic loads occur, can increase their ductility, making it possible to control ductility and displacement of concrete structures in real time.

4. Conclusion

According to this investigation the following conclusions are drawn.

1. With increase in silica sand, concrete compressive strength increases, where the maximum increase for 7-day and 28-day concrete was 11.8 % and 8.4 %, respectively, as to the highest silica sand content used in the present study, 10 %.
2. The rate of increase in concrete compressive strength due to adding silica sand is more significant during the first 7 days after fabrication. However, it seems, as to high silica contents this rate would be larger for 28-day silica sand concrete.
3. The effectiveness of AMF in enhancing compressive strength of 7-day concrete is more significant compared to 28-day one
4. Exposing hardened silica sand concrete to AMF is far more effective in enhancing compressive strength than magnetizing fresh concrete.
5. Adding 10 % silica sand and post-magnetizing concrete reduces CO₂ emissions, which is a greenhouse gas, while enhancing compressive strength by about 21 %.
6. With increase in silica content in concrete, AMF can better improve concrete compressive strength, where maximum increases for 7-day and 28-day silica sand concrete were 15 and 12.3 %, respectively, which resulted from adding 10 % silica sand.
7. Applying AMF to 10 % silica sand concrete has benefits according to ACI [49], namely:
 - Reducing minimum tensile reinforcement ratio in RC beams down to 6 %.
 - Improving RC beam ductility
 - Enhancing moment strength of RC beams

Post-magnetization makes it possible to take control of stress-strain relationship in silica sand concrete elements, opening a new window towards establishing a new generation of smart structures.

5. Acknowledgements

The authors are thankful to Mr I. Abavisani, post graduate from Semnan University for practical guidance in carrying out this study. They also like to appreciate cooperation from Mr A. Firuzbakht, the laboratory technician at civil engineering department of Semnan University, and Mr H. Ghalenoei, the president of Danesh Pajooohan Paya institution and the head of the Electric Machines laboratory of Hakim Sabzevari University.

Funding: This research did not receive any specific grant from funding agencies in the public, commercial, or not-for-profit sectors.

References

1. Alexander, M., Magee, B. Durability performance of concrete containing condensed silica fume. *Cement and Concrete Research*. 1999. 29(6). Pp. 917–922. DOI: 10.1016/S0008-8846(99)00064-2
2. Detwiler, R.J., Mehta, P.K. Chemical and physical effects of silica fume on the mechanical behavior of concrete. *ACI Structural Journal*. 1989. 86(6). Pp. 609–614.
3. Björnström, J., Martinelli, A., Matic, A., Börjesson, L., Panas, I. Accelerating effects of colloidal nano-silica for beneficial calcium-silicate-hydrate formation in cement. *Chemical Physics Letters*. 2004. 392(1–3). Pp. 242–248. DOI: 10.1016/j.cplett.2004.05.071
4. Li, H., Xiao, H., Yuan, J., Ou, J. Microstructure of cement mortar with nano-particles. *Composites Part B: Engineering*. 2004. 35(2). Pp. 185–189. DOI: 10.1016/S1359-8368(03)00052-0.

5. Lee, S.-J. Synthesis and hydration study of Portland cement components prepared by organic steric entrapment method. *Materials and Structures*. 2004. 38(275). Pp. 87–92. DOI: 10.1617/14018.
6. Lin, D.F., Lin, K.L., Chang, W.C., Luo, H.L., Cai, M.Q. Improvements of nano-SiO₂ on sludge/fly ash mortar. *Waste Management*. 2008. 28(6). Pp. 1081–1087. DOI: 10.1016/j.wasman.2007.03.023.
7. Wang, J., Du, P., Zhou, Z., Xu, D., Xie, N., Cheng, X. Effect of nano-silica on hydration, microstructure of alkali-activated slag. *Construction and Building Materials*. 2019. 220. Pp. 110–118. DOI: 10.1016/j.conbuildmat.2019.05.158.
8. Assaedi, H., Shaikh, F.U.A., Low, I.M. Influence of mixing methods of nano silica on the microstructural and mechanical properties of flax fabric reinforced geopolymer composites. *Construction and Building Materials*. 2016. 123. Pp. 541–552. DOI: 10.1016/j.conbuildmat.2016.07.049.
9. Louis, M.A. Strength of reactive silica sand powder concrete made of local powders. *Journal for Engg. Science*. 2010. 3.
10. Abd El-Baky, S., Yehia, S., Khalil, I.S. Influence of Nano Silica Addition on Properties of fresh & hardened Cement Mortar. *Housing & Building National Research Center, Cairo*. 2013.
11. Reddy, B.S.K., Ghorpade, V.G., Rao, H.S. Effect of magnetic field exposure time on workability and compressive strength of magnetic water concrete. *Int. J. Adv. Eng. Technol.* 2013. 4(3). Pp. 120–122.
12. Cai, R., Yang, H., He, J., Zhu, W. The effects of magnetic fields on water molecular hydrogen bonds. *Journal of Molecular Structure*. 2009. 938(1–3). Pp. 15–19. DOI: 10.1016/j.molstruc.2009.08.037.
13. Soltani-Todoshki, A.R., Raeisi-Vanani, H., Shayannejad, M., Ostad-Ali-Askari, K. Effects of magnetized municipal effluent on some chemical properties of soil in furrow irrigation. *Int. J. Agric. Crop Sci.* 2015. 8(3). Pp. 482–489.
14. Ahmed, H.I. Behavior of magnetic concrete incorporated with Egyptian nano alumina. *Construction and Building Materials*. 2017. 150. Pp. 404–408. DOI: 10.1016/j.conbuildmat.2017.06.022.
15. Khorshidi, N., Ansari, M., Bayat, M. An investigation of water magnetization and its influence on some concrete specificities like fluidity and compressive strength. *Computers and Concrete*. 2014. 13(5). Pp. 649–657. DOI: 10.12989/cac.2014.13.5.649.
16. Su, N., Wu, Y.-H., & Mar, C.-Y. Effect of magnetic water on the engineering properties of concrete containing granulated blast-furnace slag. *Cement and Concrete Research*. 2000. 30. Pp. 599–605.
17. Gholizadeh, M., Arabshahi, H. The Effect of Magnetic Water on Strength Parameters of Concrete. *Research Journal of Applied Sciences*. 2011. 6(1). Pp. 66–69. DOI: 10.3923/rjasci.2011.66.69.
18. Su, N., Wu, C.-F. Effect of magnetic field treated water on mortar and concrete containing fly ash. *Cement and Concrete Composites*. 2003. 25(7). Pp. 681–688. DOI: 10.1016/S0958-9465(02)00098-7.
19. Bharath, S., Subraja, S., & Kumar, P.A. Influence of magnetized water on concrete by replacing cement partially with copper slag. *Journal of Chemical and Pharmaceutical Sciences*. 2016. 9(4).
20. Gholhaki, M., Kheyroddin, A., Hajforoush, M., Kazemi, M. An investigation on the fresh and hardened properties of self-compacting concrete incorporating magnetic water with various pozzolanic materials. *Construction and Building Materials*. 2018. 158. Pp. 173–180. DOI: 10.1016/j.conbuildmat.2017.09.135.
21. Ghorbani, S., Gholizadeh, M., de Brito, J. Effect of Magnetized Water on the Mechanical and Durability Properties of Concrete Block Pavers. *Materials*. 2018. 11(9). Pp. 1647. DOI: 10.3390/ma11091647.
22. Nair S.D., F.R.D. Set-on-demand concrete. *Cement and Concrete Research*. 2014. 57. Pp. 13–27. DOI: 10.1016/j.cemconres.2013.12.001
23. Soto-Bernal, J.J., Gonzalez-Mota, R., Rosales-Candelas, I., Ortiz-Lozano, J.A. Effects of Static Magnetic Fields on the Physical, Mechanical, and Microstructural Properties of Cement Pastes. *Advances in Materials Science and Engineering*. 2015. 2015. Pp. 1–9. DOI: 10.1155/2015/934195.
24. Ko, J.M., Ni, Y.Q. Technology developments in structural health monitoring of large-scale bridges. *Engineering Structures*. 2005. 27(12). Pp. 1715–1725. DOI: 10.1016/j.engstruct.2005.02.021.
25. Chang, P.C., Flatau, A., Liu, S.C. Review Paper: Health Monitoring of Civil Infrastructure. *Structural Health Monitoring: An International Journal*. 2003. 2(3). Pp. 257–267. DOI: 10.1177/1475921703036169.
26. Abdulridha, A., Palermo, D., Foo, S., Vecchio, F.J. Behavior and modeling of superelastic shape memory alloy reinforced concrete beams. *Engineering Structures*. 2013. 49. Pp. 893–904. DOI: 10.1016/j.engstruct.2012.12.041.
27. Shin, M., Andrawes, B. Experimental investigation of actively confined concrete using shape memory alloys. *Engineering Structures*. 2010. 32(3). Pp. 656–664. DOI: 10.1016/j.engstruct.2009.11.012.
28. Deng, Z., Li, Q., Sun, H. Behavior of concrete beam with embedded shape memory alloy wires. *Engineering Structures*. 2006. 28(12). Pp. 1691–1697. DOI: 10.1016/j.engstruct.2006.03.002.
29. Wen, S., Chung, D.D.L. Piezoelectric cement-based materials with large coupling and voltage coefficients. *Cement and Concrete Research*. 2002. 32(3). Pp. 335–339. DOI: 10.1016/S0008-8846(01)00682-2.
30. Tawie, R., Lee, H.K. Piezoelectric-based non-destructive monitoring of hydration of reinforced concrete as an indicator of bond development at the steel-concrete interface. *Cement and Concrete Research*. 2010. 40(12). Pp. 1697–1703. DOI: 10.1016/j.cemconres.2010.08.011.
31. Voutetaki, M.E., Papadopoulos, N.A., Angeli, G.M., Providakis, C.P. Investigation of a new experimental method for damage assessment of RC beams failing in shear using piezoelectric transducers. *Engineering Structures*. 2016. 114. Pp. 226–240. DOI: 10.1016/j.engstruct.2016.02.014.
32. Leung, C.K.Y., Wan, K.T., Inaudi, D., Bao, X., Habel, W., Zhou, Z., Ou, J., Ghandehari, M., Wu, H.C., Imai, M. Review: optical fiber sensors for civil engineering applications. *Materials and Structures*. 2015. 48(4). Pp. 871–906. DOI: 10.1617/s11527-013-0201-7
33. Perry, M., Yan, Z., Sun, Z., Zhang, L., Niewczas, P., Johnston, M. High stress monitoring of prestressing tendons in nuclear concrete vessels using fibre-optic sensors. *Nuclear Engineering and Design*. 2014. 268. Pp. 35–40. DOI: 10.1016/j.nucengdes.2013.12.038
34. Uva, G., Porco, F., Fiore, A., Porco, G. Structural monitoring using fiber optic sensors of a pre-stressed concrete viaduct during construction phases. *Case Studies in Nondestructive Testing and Evaluation*. 2014. 2. Pp. 27–37. DOI: 10.1016/j.csndt.2014.06.002
35. Li, H.-N., Li, D.-S., Song, G.-B. Recent applications of fiber optic sensors to health monitoring in civil engineering. *Engineering Structures*. 2004. 26(11). Pp. 1647–1657. DOI: 10.1016/j.engstruct.2004.05.018.
36. Zhang, X.W., Tao, Z., Qian, Z.Y. Experimental study on the energy absorption of porous materials filled with magneto-rheological fluid. *International Journal of Impact Engineering*. 2019. 133. Pp. 103347. DOI: 10.1016/j.ijimpeng.2019.103347.
37. Abavisani, I., Rezaifar, O., Kheyroddin, A. Alternating Magnetic Field Effect on Fine-aggregate Concrete Compressive Strength. *Construction and Building Materials*. 2017. 134. Pp. 83–90. DOI: 10.1016/j.conbuildmat.2016.12.109.

38. Abavisani, I., Rezaifar, O., Kheyroddin, A. Magneto-Electric Control of Scaled-Down Reinforced Concrete Beams. *ACI Structural Journal*. 2017. 114(1). DOI: 10.14359/51689452.
39. Rezaifar, O., Abavisani, I., Kheyroddin, A. Magneto-Electric Active Control of Scaled-Down Reinforced Concrete Columns. *ACI Structural Journal*. 2017. 114(5). DOI: 10.14359/51700790.
40. Abavisani, I., Rezaifar, O., Kheyroddin, A. Alternating Magnetic Field Effect on Fine-Aggregate Steel Chip-Reinforced Concrete Properties. *Journal of Materials in Civil Engineering*. 2018. 30(6). Pp. 04018087. DOI: 10.1061/(ASCE)MT.1943-5533.0002267.
41. Rezaifar, O., Kheyroddin, A., Abavisani, I. Prospect of Magneto-Electric Active Control for Smart Concrete Structures. *Smart Nanoconcretes and Cement-Based Materials*. 1st Editio . Elsevier, 2019. Pp. 1–25.
42. ASTM C33 / C33M-18, Standard Specification for Concrete Aggregates, ASTM International, West Conshohocken, PA, 2018, www.astm.org. DOI:10.1520/C0033_C0033M-18.
43. ASTM C143 / C143M-15a, Standard Test Method for Slump of Hydraulic-Cement Concrete, ASTM International, West Conshohocken, PA, 2015, www.astm.org.
44. ASTM C39 / C39M-18, Standard Test Method for Compressive Strength of Cylindrical Concrete Specimens, ASTM International, West Conshohocken, PA, 2018, www.astm.org.
45. Firoozmakan, S., Ramezani-pour, A., Ebadi, T., Bahrami, H. Effects of Nano-Silica on Mechanical Properties and Durability of Concrete. *Journal of Civil and Environmental Engineering*. 2012. 42.1(66). Pp. 35–45.
46. Iacovacci, V., Lucarini, G., Ricotti, L., Menciassi, A. Magnetic Field-Based Technologies for Lab-on-a-Chip Applications. *Lab-on-a-Chip Fabrication and Application*. InTech, 2016.
47. Mahasenan, N., Smith, S., Humphreys, K. The Cement Industry and Global Climate Change Current and Potential Future Cement Industry CO₂ Emissions. *Greenhouse Gas Control Technologies – 6th International Conference*. Elsevier, 2003. Pp. 995–1000.
48. Nisbet, M., Vangeem, M.G., Gajda, J., Marceau, M. Environmental life cycle inventory of portland cement concrete. *Portland Cement Association*, 2002.
49. ACI318-14, Building Code Requirements for Structural Concrete and Commentary (ACI 318R-14), American Concrete Institute, Farmington Hills, MI, USA, 2014.
50. Hognestad, E., Hanson, N.W., McHenry, D. Concrete stress distribution in ultimate strength design. *ACI Structural Journal*. 1995. 52(6). Pp. 455–479.
51. Ganesan, N., Indira, P.V., Sabeena, M.V. Behaviour of hybrid fibre reinforced concrete beam–column joints under reverse cyclic loads. *Materials & Design (1980-2015)*. 2014. 54. Pp. 686–693. DOI: 10.1016/j.matdes.2013.08.076.
52. Pendyala, R., Mendis, P., Patnaikuni, I. Full-range behavior of high-strength concrete flexural members: comparison of ductility parameters of high and normal-strength concrete members. *ACI Structural Journal*. 1996. 93(1). Pp. 30–35.

Contacts:

Alireza Safari Tarbozagh, asafari@semnan.ac.ir

Omid Rezaifar, orezayfar@semnan.ac.ir

Majid Gholhaki, mgholhaki@semnan.ac.ir

© Safari Tarbozagh, A., Rezaifar, O., Gholhaki, M., 2021